

Deviations from Matthiessen's Rule in Dilute Gold and Platinum Alloys*†

R. G. STEWART‡

Argonne National Laboratory, Argonne, Illinois 60439 and Illinois Institute of Technology, Chicago, Illinois 60616

AND

R. P. HUEBENER

Argonne National Laboratory, Argonne, Illinois 60439

(Received 28 April, 1967; revised manuscript received 1 December, 1969)

The electrical resistivity of dilute alloys of gold with Ag, Cu, Pt, and Co and of platinum with Au and Rh has been measured, together with the resistivity of the pure solvent metals, between 1.6 and 373°K. The solute concentration ranged, in general, between 0.1 and 5 at.%. Also the resistivity change caused by quenched-in lattice vacancies in platinum has been measured between 1.6 and 295°K. A data analysis method has been used which eliminates the sensitivity of the results to the geometrical factor of the sample. In all systems, positive deviations $\Delta(T)$ from Matthiessen's rule are observed. For the alloys Au-Co and Pt-Rh, $\Delta(T)$ is found to be proportional to $\ln T$ between 30 and 200°K. For the other systems, the $\Delta(T)$ curves can be described approximately by a Kohler-Sondheimer-Wilson equation. At low temperatures, the temperature dependence of Δ is found to be somewhat lower than that of the resistivity of the pure solvent metal. For the low solute concentrations, a sharp peak in the $\Delta(T)$ curves at about 30–50°K is observed. Various possibilities for explaining the results are discussed, including the two-band model, the anisotropy of the electron scattering, and the shift in the Fermi surface due to alloying.

I. INTRODUCTION

OVER 100 years ago, Matthiessen^{1,2} noted that the temperature dependence of the electrical resistance of a wide range of dilute alloys was the same as that of the host solvent metal. His measurements were carried out between the ice point and the boiling point of water. He found that the effect of adding solute elements was to add a resistance which depended on the solute concentration c , but not on the temperature T . This result can be expressed as

$$\rho_{\text{alloy}}(c, T) = \rho_{\text{solvent}}(T) + \rho_{\text{solute}}(c). \quad (1)$$

Equation (1) was found to apply to most alloy systems to a surprising degree of accuracy and became known as Matthiessen's rule (MR). It implies that the scattering by the thermal motion of the lattice and by the impurity are independent and additive.

As measurements were extended to lower and lower temperatures, Eq. (1) was not so well obeyed, as Grüneisen³ was the first to emphasize. To take into account the discrepancy, another term must be added to Eq. (1) representing the temperature dependence of the impurity resistance, $\Delta(c, T)$, which is known as the deviation from Matthiessen's rule. Equation (1) then becomes

$$\rho_{\text{alloy}}(c, T) = \rho_{\text{solvent}}(T) + \rho_{\text{solute}}(c, 0) + \Delta(c, T). \quad (2)$$

* Based on work performed under the auspices of the U. S. Atomic Energy Commission.

† This paper is based in part on a dissertation submitted by R. G. Stewart to the Graduate School of the Illinois Institute of Technology in partial fulfillment of the requirements for the Ph.D. degree.

‡ Present address: Lockheed Palo Alto Research Laboratory, Palo Alto, Calif. 94304.

¹ A. Matthiessen, Ann. Physik. Chem. 110, 190 (1860).

² A. Matthiessen and C. Vogt, Ann. Physik. Chem. 122, 19 (1864).

³ E. Grüneisen, Ann. Physik 5, 530 (1933).

The ratio $\Delta(c, T)/\rho_{\text{solute}}(c, 0)$ is usually small, on the order of several percent. Furthermore, the temperature dependence of the deviations in the room-temperature range is frequently quite small, so that Matthiessen's observation $(d\rho/dT)_{\text{alloy}} = (d\rho/dT)_{\text{solvent}}$ is remarkably valid in that temperature range. (Clearly, he was done a disservice when others extended his rule to all temperatures.)

The early measurements⁴ of the deviations from MR established that $\Delta(c, T)$ increases with temperature and then saturates, and that it increases with solute concentration. A function having this general behavior was derived by Sondheimer and Wilson⁵ on the presumption that two bands, s and d , contribute to the conductivity, and that the conductivities of the two bands add. Then the presumption is made that MR applies to each band separately; i.e., the impurity and lattice resistivities add within one band and $\Delta_s(T) = \Delta_d(T) = 0$. Next, using the standard rules for evaluating the resistance of a series-parallel combination, an *apparent* temperature dependence of the impurity resistance or deviation from MR appears having the general form

$$\frac{1}{\Delta(T)} = \frac{1}{\beta\rho_{\text{solute}}(0)} + \frac{1}{\gamma\rho_{\text{solvent}}(T)}. \quad (3)$$

Here β and γ are constants related to the conductivities in the bands.

Later Kohler⁴ derived an expression for $\Delta(T)$ of precisely the same form as (3), but based on different and more general premises. Kohler found the solution of the Boltzmann equation under the applied external field for the case of two simultaneous collision operators,

⁴ M. Kohler, Z. Physik 126, 495 (1949), and references therein.

⁵ E. H. Sondheimer and A. H. Wilson, Proc. Roy. Soc. (London) 190, 435 (1947).

representing the impurity scattering and the thermal lattice scattering, respectively, by using the Ritz variational method together with trial distribution functions which solve the problem exactly when the collision operators act separately. The resulting total resistivity exceeds the sum of the contribution of each operator acting alone, yielding a deviation from MR of the form of Eq. (3), *even in the simplest case of one isotropic spherical conduction band*. In the following, Eq. (3) will be referred to as the Kohler-Sondheimer-Wilson (KSW) equation. The KSW equation is relatively successful in predicting the general temperature and concentration dependence of the measured deviations from MR.

Using Kohler's general method, Sondheimer⁶ obtained expressions for the electrical conductivity, thermal conductivity, and thermoelectric power as a function of temperature in terms of high-order determinantal expansions. Relative to an "ideal" conductivity described by a Bloch-Grüneisen relation, he found that the conductivity of both a pure and impure specimen are increased, but that the amount of increase is smaller for a highly impure than a less impure sample. This yields a positive deviation from MR that has a maximum at low temperatures and vanishes at high temperatures. This effect was employed by Krautz and Schultz⁷ to explain a peak in $\Delta(T)$ at about 60°K observed in Ag-0.6Au and Au-1.0Ag alloys.⁸ They used the KSW equation to fit the balance of the $\Delta(T)$ curve after the peak contribution was subtracted off.

Magnetic impurities can cause a deviation $\Delta(T)$ which appears as a minimum in the resistivity at very low temperatures, say 5 to 20°K.⁹⁻¹¹ The temperature and concentration dependence of this effect has been explained by Kondo¹² as an interaction between conduction electron pairs coupled by spin flipping due to the impurity magnetic moment. As will be seen in the present paper, and as was pointed out by Hedgcock and Muir,¹³ for some transition metal solutes $\Delta(T)$ varies logarithmically with temperature, suggesting that the spin term is important in the resistivity at higher temperatures than usually expected. The magnitude of the deviations are generally larger for transition metal solutes than for nontransition metal solutes.

⁶ E. H. Sondheimer, Proc. Roy. Soc. (London) **A203**, 75 (1950).

⁷ E. Krautz and H. Schultz, Z. Naturforsch. **12a**, 710 (1957).

⁸ The notation employed here says that the first-named element is the major constituent or solvent; the number gives the concentration in atomic percent of the second-named minor constituent or solute.

⁹ A. N. Gerritsen and J. O. Linde, Physica **18**, 877 (1952).

¹⁰ G. J. van den Berg, in *Progress in Low Temperature Physics*, edited by C. J. Gorter (North Holland Publishing Co., Amsterdam 1964), Vol. IV, p. 194.

¹¹ G. J. van den Berg, in *Proceedings of the Ninth International Conference on Low Temperature Physics*, edited by J. G. Daunt, D. O. Edwards, F. J. Mueller, and M. Yaqub (Plenum Press, New York, 1965), Vol. B, p. 955.

¹² J. Kondo, Progr. Theoret. Phys. (Kyoto) **32**, 37 (1964); **34**, 372 (1965).

¹³ F. T. Hedgcock and W. B. Muir, Phys. Rev. **136**, A561 (1964).

Anisotropy of the relaxation time for phonon and impurity scattering over the Fermi surface can give rise to a deviation from MR of the type described by the KSW equation. This would constitute an *apparent* deviation from MR, as discussed earlier. If the anisotropy of the impurity scattering relaxation time is also temperature dependent, we have a *real* deviation from MR imbedded in the apparent deviation.

The effect of the thermal motion of an impurity ion (without perturbing the usual thermal motion of the pure lattice) in directly causing a temperature-dependent scattering or $\Delta(T)$ has been treated by Koshino,^{14,15} Klemens,^{16,17} and Taylor.^{18,19} Koshino's result, from second-order perturbation theory using a screened Coulomb impurity potential, gave $\Delta(T)$ proportional to the square of the valence difference, to the impurity concentration, and to the square of the temperature. Taylor considered the problem diagrammatically and showed that a group of second-order processes cancel the first-order processes of Koshino so that the resulting deviation is much smaller. Klemens suggested the motion of the impurity *relative to its neighbors* would give a local lattice strain energy causing a deviation $\Delta(T)$ proportional to T^4 at very low temperatures.

Langer²⁰ employed Kubo's fluctuation-dissipation theory of irreversible processes to investigate the impurity resistance of a Fermi electron gas at finite temperatures. He finds that the lowest order correction terms cancel, leaving only a term due to correlation of quasiparticles which is independent of impurity concentration and, hence, does not contribute to deviations from MR.

The introduction of an impurity atom into a lattice can change the vibrational characteristics of the lattice and, hence, those aspects of a physical quantity which are determined by the phonon spectrum. This general problem has been extensively discussed in recent years.^{21,22} The effect of alloying on the specific heat²³⁻²⁵ clearly demonstrates the change in the vibrational

¹⁴ S. Koshino, Progr. Theoret. Phys. (Kyoto) **24**, 484 (1960); **24**, 1049 (1960).

¹⁵ S. Koshino, Progr. Theoret. Phys. (Kyoto) **33**, 154 (1965).

¹⁶ P. G. Klemens, J. Phys. Soc. Japan **18**, Suppl. II, 77 (1963).

¹⁷ D. H. Damon and P. G. Klemens, in *Proceedings of the Ninth International Conference on Low Temperature Physics*, edited by J. G. Daunt, D. O. Edwards, F. J. Mueller, and M. Yaqub (Plenum Press, New York, 1965), Vol. B, p. 996.

¹⁸ P. L. Taylor, Proc. Phys. Soc. (London) **80**, 755 (1962).

¹⁹ P. L. Taylor, Phys. Rev. **135**, A1333 (1964).

²⁰ J. S. Langer, Phys. Rev. **127**, 5 (1962).

²¹ A. A. Maradudin, in *Solid State Physics*, edited by F. Seitz and D. Turnbull (Academic Press Inc., New York, 1966), Vol. 18, p. 273.

²² M. Yussouff and J. Mahanty, Proc. Phys. Soc. (London) **87**, 689 (1965); **85**, 1223 (1965).

²³ Yu. Kagan and Ya. Iosilevskii, Zh. Eksperim. i Teor. Fiz. **45**, 819 (1963) [English transl.: Soviet Phys.—JETP **18**, 562 (1963)]; G. Kh. Panova and B. N. Samoilov, Zh. Eksperim. i Teor. Fiz. **49**, 456 (1965) [English transl.: Soviet Phys.—JETP **22**, 320 (1966)].

²⁴ H. Culbert and R. P. Huebener, Phys. Letters **24A**, 530 (1967).

²⁵ J. A. Cape, G. W. Lehman, W. V. Johnston, and R. E. de Wames, Phys. Rev. Letters **16**, 892 (1966).

spectrum besides the change in the electronic density of states. Goodman²⁶ has investigated the change in the structure factor over wide ranges of binary alloy composition. Schlup²⁷ has calculated the frequency spectrums for disordered lattices as a function of mass ratio and of concentration.

The anisotropy of the lattice vibrational spectrum has been shown by Bross,²⁸ using Kohler's variational procedure and the Sommerfeld-Bethe transition probability formalism, to lead to a deviation from MR which is similar to the KSW equation.

The change in the Debye temperature with alloying has been suggested as the cause of deviations from MR by Hedgcock and Muir²⁹ and by Gerritsen and Das.²⁹ Damon and Klemens³⁰ have looked for the effects of local modes on $\Delta(T)$ in gold alloys without success. Huebener³¹ has shown that there is a small contribution to deviations from MR caused by phonon drag effects. This contribution has a peak at low temperatures. The calculated size of the phonon drag effect is one to two orders of magnitude smaller than the actually observed peak in the deviations from MR.

Recently, Kagan and Zhernov³² have treated the deviations from MR in the electrical resistivity of metals with nonmagnetic impurities using the diffraction model for describing the electron scattering within a lattice. Their theory takes into account consistently the deformation of the phonon spectrum due to the introduction of impurity atoms and also the change in the scattering potential at the site of the impurity.

Dugdale and Basinski³³ and Matsuda³⁴ have recently used the two band model, the KSW equation, and the anisotropy of the electron relaxation time over the Fermi surface to treat deviations from MR and the Hall coefficient in dilute alloys as a function of temperature. Extending Ziman's³⁵ eight-cone Fermi-surface model of belly and neck electrons, they explain their results in a plausible and self-consistent manner.

Damon, Mathur, and Klemens³⁶ investigated the deviations from MR in dilute gold alloys below 40°K, and divided them into a two-band model term, and a term approximately proportional to T^4 resulting from the deformation of the impurity potential due to the strain of the lattice in the neighborhood of the impurity. Detailed comparisons of our results with specific aspects

²⁶ P. L. Leath and B. Goodman, *Phys. Rev.* **148**, 968 (1966).

²⁷ W. A. Schlup, *Physik Kondensierten Materie* **3**, 227 (1965).

²⁸ H. Bross, *Z. Naturforsch.* **14a**, 560 (1959).

²⁹ S. B. Das and A. N. Gerritsen, *Phys. Rev.* **135**, A1081 (1964).

³⁰ D. H. Damon and P. G. Klemens, *Phys. Rev.* **138**, A1390 (1965).

³¹ R. P. Huebener, *Phys. Rev.* **146**, 502 (1966).

³² Yu. Kagan and A. P. Zhernov, *Zh. Eksperim. i Teor. Fiz.* **50**, 1107 (1966) [English transl.: *Soviet Phys.—JETP* **23**, 737 (1966)].

³³ J. S. Dugdale and Z. S. Basinski, *Phys. Rev.* **157**, 552 (1967).

³⁴ Takeshi Matsuda, *J. Phys. Chem. Solids* **30**, 859 (1969).

³⁵ J. M. Ziman, *Phys. Rev.* **121**, 1320 (1961); V. Heine, *Phil. Mag.* **12**, 53 (1965).

³⁶ D. H. Damon, M. P. Mathur, and P. G. Klemens, *Phys. Rev.* **176**, 876 (1968).

of their approach will be made below in the text of the paper.

Scattering by the surface in thin wires and foils has been found to produce deviations from MR. A review of these phenomena has been given recently by Brändli and Olsen.³⁷

Panova, Zhernov, and Kutaitshev³⁸ recently observed a pronounced maximum in $\Delta(T)$ around 55°K in dilute Mg-Pb alloys. They explained this maximum by pseudo-localized modes associated with the Pb ions. Panova and Samoilov³⁸ measured the effect of isotopic mass on the resistivity of pure cadmium. They found heavy isotope samples had a higher temperature dependence of the resistivity below 100°K than did light isotope samples. This result was ascribed to the increased density of the low frequency portion of the phonon spectrum which is of greater significance to the electron-phonon scattering at very low temperatures.

In the present paper the deviations from MR in dilute gold and platinum alloys are measured for the temperature range between 1.6 and 373°K. The solute concentration in the alloys varies in general between 0.1 and 5 at.-%. The deviations from MR for vacancies in Pt, introduced by quenching, are measured between 1.6 and 295°K. Section II gives a description of the experimental techniques. In Sec. III a method for analyzing the data is presented which eliminates the sensitivity of the results to the geometrical factors of the samples without introducing any additional assumptions on the temperature dependence of $\Delta(T)$. The experimental results, and comparisons with previous work, are given in Sec. IV. A discussion of the results is given in Sec. V.

II. EXPERIMENTAL PROCEDURE

Sample Holder and Cryostat

The sample holder, as shown in Fig. 1, is suspended by thin-wall perforated stainless steel tubing from a

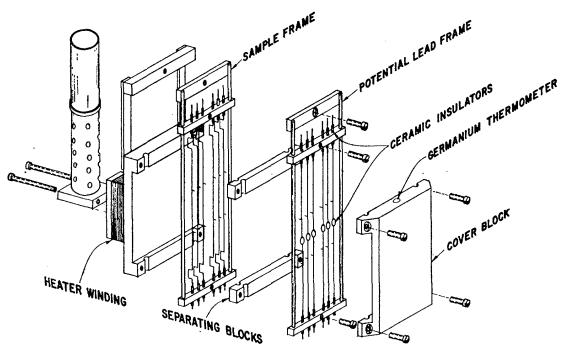


FIG. 1. Exploded perspective view of cryostat sample holder.

³⁷ G. Brändli and J. L. Olsen, *Mater. Sci. Eng.* **4**, 61 (1969).

³⁸ G. Kh. Panova, A. P. Zhernov, and V. I. Kutaitshev, *Zh. Eksperim. i Teor. Fiz.* **53**, 423 (1967) [English transl.: *Soviet Phys.—JETP* **26**, 283 (1968)]; G. K. Panova and B. N. Samoilov, *ibid.* **53**, 1539 (1967) [English transl.: *ibid.* **26**, 888 (1968)].

refrigerant well in the top of the cryostat. A copper plug sealing the bottom of the well serves as the thermal reference for the thermocouple junction. A bifilar 200- Ω 5-mil manganin heater wire is wound around a copper block which is designed to provide a symmetric heat path to the samples. Six sample wires (five alloy wires plus one wire of the pure solvent metal) are electrically insulated from the block by cigarette paper varnished on the block with GE No. 7031 varnish. A frame holding 12 potential wire connections is mounted parallel to the sample frame and separated from it by two insulated copper blocks. A copper block, containing the germanium resistance thermometer, closes the assembly. Copper side plates act as radiation shields.

Electrical connections from the cryostat to the external circuitry are made with eight 10-mil and 11 5-mil copper wires, plus one 2.5-mil Au -2.1 Co thermocouple wire. These wires are clamped underneath two copper plates against the lower external surface of the heater block in order to equilibrate them at the copper block temperature prior to bringing them to the samples. In this way heat leakage from the sample wires is prevented.

The cryostat is closed by a (ribbed) copper can with a Wood's metal seal. During the measurements the system is evacuated to less than 10^{-4} Torr. Below 77°K the cryostat is immersed in liquid helium. For measurements at higher temperatures either liquid nitrogen, ice water, or heated water is used as a temperature bath.

Sample Description and Preparation

Most measurements were made on 10-mil polycrystalline wires obtained from commercial sources.³⁹ The solute concentrations of the alloys were ascertained by wet chemical and neutron activation analyses. The purity of the alloys and of the pure comparison wires with respect to minor constituents was about 10 parts per million for the platinum samples and two parts per million for the gold samples. The wires were rinsed in dilute nitric acid for 20 min, distilled water, and pure alcohol prior to spotwelding into the sample frame. The platinum (gold) wires were annealed by Joule heating in air using direct current according to a schedule starting at about 1500°C (950°C) and ending with a 24-h period at 900°C (750°C). Finally, they were cooled to room temperature within one hour. The resistivity ratios $\rho(296°K)/\rho(4.2°K)$, obtained for the pure platinum wires were in the range 4400 to 7400, while for the pure gold wires the range was 1100 to 1400.

In the experiments with quenched Pt, the Pt wire was heated to the desired prequench temperature by passing a direct current through it. The heated wire was then plunged into ice water with a quench rate of 5×10^4 °C/

³⁹ The Pt-Au and the Au-Pt alloys were made by Baker-Engelhard, Inc., Newark, N. J. The Au-Ag and Au-Cu alloys and the pure Au specimen were made by Cominco American, Inc., Spokane, Wash. The Au-Co, Pt-Rh, pure Pt, and one Au-Ag specimen were made by Sigmund Cohn, Inc., Mt. Vernon, N. Y.

sec. The quenching technique has been described elsewhere.⁴⁰ The quenched samples were mounted in the cryostat and cooled to liquid nitrogen temperatures within 90 min after quenching. The imperfections introduced into Pt by quenching are the excess concentration of lattice vacancies existing in thermal equilibrium at the high prequench temperature. By the rapid cooling the lattice vacancies are frozen into the lattice. In platinum no annealing of quenched-in vacancies occurs at room temperature.⁴¹

The specific characteristics of the alloys investigated are summarized in Tables I and II of Sec. IV.

The potential contacts were 2-mil pure gold or platinum wires spotwelded to the sample and the potential leads after annealing of the specimen wires. These welds were made after the sample frame and the potential lead frame were bolted together. Small offset bends were formed into each end of the sample wires to promote temperature uniformity during annealing, and to minimize strain from mechanical stresses. The ends of the sample wires were spotwelded to 20-mil gold or platinum leads that passed through ceramic insulators and were cemented to the sample holder.

Measurement System

For the resistance measurements conventional potentiometric techniques were used. The voltage measurements were taken with a Honeywell-Rubicon Model 2768 six-dial potentiometer. A Princeton Applied Research Model TC100.2BR regulated power supply provided a stable 30-mA sample current. The current drift was less than 4 parts per million over several days. A Keithley Model 147 null detector provided better than 0.01- μ V resolution for the potentiometer. The effects of thermal emf's on the calculated sample resistance were eliminated by reversing the current. To enable rapid and convenient current reversal without introducing an asymmetric current increment, a special reversing switch was made employing four Potter and Brumfield Model JML-5430-82 mercury-wetted contact relays controlled by two latching relays. The contact resistance of the mercury-wetted relays was found to be far more stable and reproducible than dry contact switches or relays. By using the mercury-wetted relays, and their driver relays, in a latching mode of operation no thermal dissipation occurs in the relays except during the instant of switching; hence, effects of any thermal emf's were insignificant in the sample current circuit. Switching of the potentiometer input to the different samples and reversing the polarity were accomplished with two two-ganged, 10-position, Chicago Dynamic Industries No. TSDP10A gold-plated printed circuit switches. The thermal emf's of these simple, inexpensive switches were less than 0.01 μ V.

⁴⁰ R. P. Huebener, Phys. Rev. 135, A1281 (1964).

⁴¹ J. J. Jackson, in *Proceedings of the International Conference on Lattice Defects in Quenched Metals* (Academic Press Inc., New York, 1965), p. 467.

The temperature in the cryostat was measured below 20°K with a Honeywell MHSP2401 germanium thermometer and above 20°K with a *Au*-2.1Co versus Cu thermocouple. The voltages were measured with a Leeds & Northrup K3 potentiometer. The precision of the germanium thermometer is of the order of 0.1°K. The *Au*-Co thermocouple calibration by the NBS⁴² was employed for temperature conversion. The initial accuracy of the thermocouple was good, about 1-2%. However, in the course of the experiments, the thermocouple accuracy deteriorated somewhat. Therefore, above 20°K the electrical resistance of the pure comparison sample was used as a thermometer. For the platinum experiments, a resistivity-versus-temperature calibration of the NBS was employed; for the gold experiments, the data of Onnes⁴³ were used.

The temperatures measured with the germanium thermometer matched within $\frac{1}{4}$ deg those indicated by the thermocouple or the resistance measurements in the temperature interval of overlap (15-20°K). In the heated water bath measurements the temperatures calculated from the resistance of the pure samples agreed within $\frac{1}{2}$ deg or better with the temperature indicated by mercury immersion thermometers. The temperatures used in the final data presentation are believed to be correct in absolute value within 1 deg above 30°K, and within $\frac{1}{4}$ deg below 30°K.

A temperature stability approaching 0.001 deg was achieved in the cryostat by an inverse feedback control system that consisted of the *Au*-Co thermocouple, a Leeds and Northrup K3 potentiometer, a Keithley Model 149 millimicrovoltmeter serving as null detector, and a Hewlett-Packard/Harrison Model 6258A power supply which provided the heater current. This system attained the dynamic control plateau without overshoot or hunting, yielding temperature constancy almost two orders of magnitude better than manual control.

Data-Taking Techniques

Inherent in the data analysis method finally adopted to calculate the deviations from MR from the basic resistance information is the presumption that the resistances of the different samples are measured at the same temperature. This requires that a well-equilibrated isothermal condition in the sample holder be achieved and maintained experimentally. Using the temperature control system described above, such a condition could be achieved in 15-30 min for temperatures below 270°K. The data taken between room temperature and 373°K were obtained using an external hot circulating water bath. As long as 2 h were required to reach a satisfactory equilibrium in this case, and the degree of temperature stability was about two orders of

magnitude worse than in the measurements below 273°K. This is evident in data scatter apparent in the high-temperature results.

After equilibrium at the desired temperature was reached, the measurements were taken according to the following sequence: (1) current for both current directions, (2) sample voltage for both current directions for all samples, and (3) current for both current directions. Temperature measurements were made prior to each polarity of each current and voltage measurement. Thus the resistance of the individual samples, with respect to that of the pure comparison sample, could be corrected for current and temperature shifts by using interpolation subroutines incorporated into the FORTRAN program which computed the resistance from the raw data. The interpolation corrections to the resistivity were usually less than 0.03%.

In order to calculate the ratio of the length l of the sample to the cross-sectional area A , which ratio is known as the geometrical factor $G=l/A$, the length of the sample wires between the potential probes was measured with a traveling microscope, and the cross-sectional area was determined by weighing out sections of the wire with known length. The densities of the alloy samples were computed from known values of the lattice constants,⁴⁴ and the chemical assays of the solute concentrations. The precision of the measurements allowed determination of the geometrical factor to about $\frac{1}{2}\%$ accuracy.

The effect of thermal expansion on the pure and alloyed samples introduces a correction to the measured deviations from MR of at most 2%. This was deemed small enough to be neglected in the data analysis. The correction is this small because of the data analysis procedure employed, as discussed below. Likewise, the effect of volume expansion of the quenched samples due to the formation of lattice vacancies is negligible for the vacancy concentrations actually introduced (being approximately one-tenth the magnitude of the thermal expansion correction).

III. ANALYSIS OF DATA IN MATTHIESSEN'S-RULE EXPERIMENT

The information experimentally available is the electrical *resistance* of the various samples as a function of temperature. Matthiessen's rule deals with the difference in the electrical *resistivity* between two different samples. Thus, the geometrical factor, the ratio of the sample length to cross-sectional area, $G=l/A$, is needed for each sample to calculate resistivity differences. Small errors in the determination of the geometrical factor can lead to serious errors in the determination of $\Delta(T)$ from resistance values.⁴⁵ For the temperature

⁴² R. L. Powell, M. D. Bunch, and R. J. Corruccini, *Cryogenics* 1, 1 (1961).

⁴³ H. Kamerlingh Onnes and W. Tuyn, *International Critical Tables* (McGraw-Hill Book Co., New York, 1929), Vol. 6, p. 124.

⁴⁴ W. B. Pearson, *Handbook of Lattice Spacings and Structures of Metals and Alloys* (Pergamon Press, Inc., New York, 1958), pp. 429, 441, 820.

⁴⁵ P. Alley and B. Serin, *Phys. Rev.* 116, 334 (1959).

range in which $\rho_{\text{solvent}}(T) \gg \Delta(T)$, the errors can be very large, and furthermore introduce a fictitious temperature dependence of Δ . To circumvent this source of error, Alley and Serin,⁴⁵ as have others,⁴⁶ have normalized resistance data by dividing by the ice-point values, which cancels the geometrical factor, presuming thermal expansion effects to be negligible. In some of the normalization methods presented in the literature,^{18,47} the geometrical factors of the samples were not actually eliminated from the analysis. The normalization process of Alley and Serin makes it necessary to either know the deviations from Matthiessen's rule at the ice temperature or else the temperature dependence of the deviations in that temperature neighborhood in order to calculate the deviations over the entire temperature range. In order to obtain the deviation at the ice point, Alley and Serin introduced the additional assumption that the deviations from Matthiessen's rule are independent of temperature in the temperature interval between the ice point and the boiling point of water. It will be shown below that this assumption is not necessary to analyze the data, and moreover may be incorrect in some cases.

Following the literature motivations we normalize the resistance data by dividing by the ice-point resistance. In addition, we subtract the residual resistance in numerator and denominator for both the alloy sample and the pure sample. This yields the following quantity which is well-defined experimentally, and which is not a function of the geometrical factor, presuming thermal expansion effects to be negligible:

$$\delta_j(T) = \frac{R_j(T) - R_j(0)}{R_j(\text{ice}) - R_j(0)} - \frac{R_k(T) - R_k(0)}{R_k(\text{ice}) - R_k(0)}. \quad (4)$$

The subscripts j and k refer to the alloy and the pure comparison sample respectively.⁴⁸ Obviously, $\delta_j(0) = \delta_j(\text{ice}) = 0$. The variation of δ_j with T is shown in

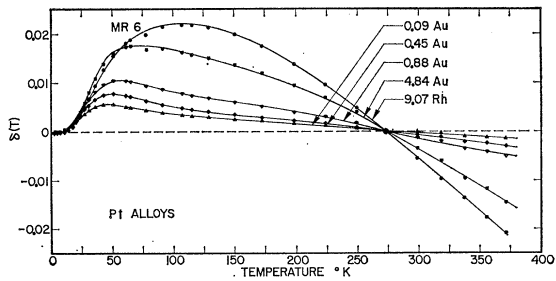


FIG. 2. Temperature dependence of $\delta_j(T)$ for the platinum alloys of run MR6.

⁴⁶ P. G. Klemens and G. C. Lowenthal, Australian J. Phys. **14**, 352 (1961).

⁴⁷ Yu. N. Tsiovkin and N. V. Volkenstein, Zh. Eksperim. i Teor. Fiz. **48**, 796 (1965) [English transl.: Soviet Phys.—JETP **21**, 527 (1965)].

⁴⁸ This choice is made to correspond to the fixed point variable naming convention of Fortran. The mnemonic k = komparison is helpful.

Fig. 2 for a series of platinum alloys. A nonzero value of $\delta_j(T)$ immediately implies a deviation from Matthiessen's rule which can be shown as follows. We have from Eq. (2)

$$\rho_j(T) = \rho_k(T) + \rho_j(0) + \Delta(T).$$

Thus, neglecting any deviations from MR for the comparison sample, $\Delta_k(T)$, Eq. (4) can be rewritten

$$\delta_j(T) = \frac{\rho_k(T) + \Delta(T)}{\rho_k(\text{ice}) + \Delta(\text{ice})} - \frac{\rho_k(T)}{\rho_k(\text{ice})} \quad (5)$$

which is a *theoretical* quantity. From Eq. (5) we see that

$$\delta_j(T) \neq 0, \quad \text{if } \Delta(T) \neq 0.$$

There are two unknowns in Eq. (5), $\Delta(T)$ and $\Delta(\text{ice})$. If $\Delta(\text{ice})$ can be determined, then $\Delta(T)$ is immediately given for all T , since the left-hand side of Eq. (5) is

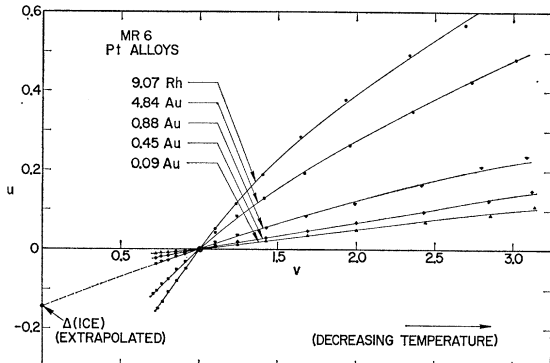


FIG. 3. (u, v) plot for the platinum alloys of run MR6.

directly known from experimental data. The terms in (5) can be rearranged into the form

$$\frac{\delta_j(T)\rho_k(\text{ice})}{\delta_j(T) + \rho_k(T)/\rho_k(\text{ice})} = \Delta(T) \frac{1}{\delta_j(T) + \rho_k(T)/\rho_k(\text{ice})} - \Delta(\text{ice}). \quad (6)$$

If we define the two known quantities

$$u(T) \equiv \frac{\delta_j(T)\rho_k(\text{ice})}{\delta_j(T) + \rho_k(T)/\rho_k(\text{ice})}$$

and

$$v(T) \equiv \frac{1}{\delta_j(T) + \rho_k(T)/\rho_k(\text{ice})},$$

Eq. (6) becomes

$$u = \Delta(T)v - \Delta(\text{ice}). \quad (7)$$

This useful equation, which will be referred to as the (u, v) equation henceforth, is the solution to the problem provided $\Delta(\text{ice})$ can be found. Since u and v are known

experimentally, v can be plotted versus u . A set of (u, v) loci for several platinum alloys is shown in Fig. 3. Because v is approximately the normalized conductivity of the comparison sample, increasing v corresponds to decreasing temperatures. The data in the figure corresponds to temperatures higher than 50°K. By virtue of the definitions of δ , u , and v , the loci for all samples will pass through the point $(0, 1)$ in the (u, v) plane. Note by inspecting (7) that, if the $\Delta(T)$ are constant in the high temperature range, the extrapolated intercept of the (u, v) loci on the u axis, $(v=0)$, is a direct measure of $\Delta(\text{ice})$. Further, we note that if $\Delta(T)$ is constant in the high-temperature range then the (u, v) loci will be a straight line with no curvature. However, it can be shown⁴⁹ that if $\rho_j(T)$, $\rho_k(T)$, and $\Delta(T)$ are linear functions of temperature that the slope of the (u, v) curve will be constant even though $\Delta(T)$ is not. This particular case corresponds to (7) representing an exact differential equation. However, in such a case the function δ as given by the experimental data and Eq. (4)

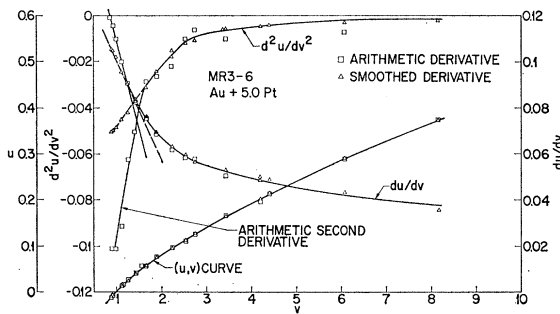


FIG. 4. (u, v) and its first and second derivatives for an $Au - 5.0$ Pt alloy illustrating effects of smoothing on higher derivatives.

should be zero for all temperatures. In no case did we actually find $\delta(T)=0$ for all T . This we interpret as due to the presence of terms of second and higher order in the resistivities. These terms essentially lift the exactness condition, and more important suggest that $\Delta(T)$ can be obtained from the slope and curvature of the (u, v) curve.

Suppose we differentiate (7) twice, yielding

$$\frac{du}{dv} = \Delta(v) + v \frac{d\Delta}{dv} \quad (8)$$

and

$$\frac{d^2u}{dv^2} = 2 \frac{d\Delta}{dv} + v \frac{d^2\Delta}{dv^2}. \quad (9)$$

These relations are useful since u , du/dv , and d^2u/dv^2 can be found from the experimental (u, v) curve either graphically, numerically, or by polynomial fitting and

⁴⁹ P. G. Klemens (private communication). The smoothing routines used in the analysis of the data were developed by R. W. Prince of Lockheed Aircraft Corporation.

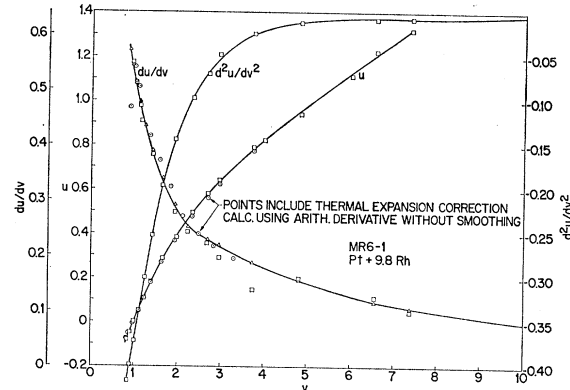


FIG. 5. (u, v) and the first two derivatives for the thermocouple alloy $Pt + 9.8$ Rh. Note the extremely small effect of an exact calculation of the thermal expansion corrections on this method of analysis.

smoothing procedures. Typical curves for $u(v)$, du/dv , and d^2u/dv^2 are shown in Figs. 4 and 5. Now focusing our attention on the variations in the (u, v) curve near the ice temperature, $T(\text{ice})$, we assume that $\Delta(v)$ can be expanded as a Taylor series using three terms in the series,

$$\Delta(v) = \Delta(\text{ice}) + \frac{(v-1)}{1!} \Delta'(\text{ice}) + \frac{(v-1)^2}{2!} \times \Delta''(\text{ice}) + \frac{(v-1)^3}{3!} \Delta'''(\text{ice}). \quad (10)$$

This expression can be differentiated twice to obtain equations for $d\Delta/dv$ and $d^2\Delta/dv^2$, which can then be substituted into (9), which, on combining terms with like powers of v , yields

$$d^2u/dv^2 = [2\Delta'(\text{ice}) - 2\Delta''(\text{ice}) + \Delta'''(\text{ice})] + v[3\Delta''(\text{ice}) - 3\Delta'''(\text{ice})] + v^2[2\Delta'''(\text{ice})].$$

This is a useful equation since the coefficients in the brackets can be obtained experimentally from the least-square polynomial expansion of the second derivative, namely,

$$d^2u/dv^2 = A_0 + A_1 v + A_2 v^2. \quad (11)$$

Therefore,

$$\Delta'''(\text{ice}) = \frac{1}{2} A_2, \quad (12)$$

$$\Delta''(\text{ice}) = \frac{1}{3} A_1 + \frac{1}{2} A_2, \quad (13)$$

$$\Delta'(\text{ice}) = \frac{1}{2} A_0 + \frac{1}{3} A_1 + \frac{1}{4} A_2. \quad (14)$$

Knowing this last quantity is the key to the problem, since $\Delta(\text{ice})$ can be deduced from (8) evaluated at the ice temperature,

$$\Delta(\text{ice}) = \frac{du}{dv} \bigg|_{T \text{ ice}} - v \frac{d\Delta}{dv} \bigg|_{T \text{ ice}}. \quad (15)$$

With $\Delta(\text{ice})$ also known it is possible to reconstruct

$\Delta(T)$ by rewriting (5) in the form

$$\Delta(T) = \delta_j(T) [\rho_k(\text{ice}) + \Delta(\text{ice})] + \frac{\Delta(\text{ice})}{\rho_k(\text{ice})} \rho_k(T). \quad (16)$$

Once $\Delta(\text{ice})$ is known, this is a definitive equation for $\Delta(T)$ since all other quantities in the equation are known experimentally. This equation will retain the full structure inherent in the data in temperature regions of rapid change since no derivatives are contained which involve data at different temperatures.

An alternative to differentiating the (u,v) curve twice as needed by the prior procedure, is to take the third-order expansion of $\Delta(v)$, (10), and substitute that into the (u,v) equation which yields an equation which is fourth order in v . In addition, one can also fit the experimental (u,v) loci with a fourth-order polynomial in v . This essentially over constrains the solution since there are four unknowns and five experimental coefficients. An internal check of the validity of the previous expansions, such as (10), consists of comparing the two values of $\Delta(\text{ice})$, which can be found by this method. If we let

$$u = A_0 + A_1 v + A_2 v^2 + A_3 v^3 + A_4 v^4 \quad (17)$$

and compare coefficients term by term with those obtained by substituting (10) into (7), we obtain

$$\Delta(\text{ice}) = -A_0, \quad (18)$$

$$\Delta'''(\text{ice}) = 6A_4,$$

$$\Delta''(\text{ice}) = 2A_3 + 6A_4,$$

$$\Delta'(\text{ice}) = A_2 + 2A_3 + 3A_4,$$

$$\Delta(\text{ice}) = A_1 + A_2 + A_3 + A_4. \quad (19)$$

By numerically comparing (18) and (19) as thus obtained from fourth-order least-square polynomial fits to the experimental (u,v) curves, the average percent difference in the $\Delta(\text{ice})$ values was 0.32% for all samples, while the largest difference was 1.5%. This suggests a high degree of internal consistency of the method.

The agreement of the $\Delta(\text{ice})$ values obtained by the derivative fitting procedure, Eqs. (10)–(15), and those obtained by fitting the (u,v) curve directly, Eqs. (17)–(19), varied from a few percent for some samples to perhaps 30% for others. The problems involved in smoothing and differentiating noisy data are non-trivial. Figure 4 shows the large difference in the first and second derivative resulting from using the basic arithmetic definition of the derivative directly, or first smoothing the raw data and obtaining the derivative from the expansion of the fitting polynomial. Smoothing and differentiating are not commuting operations. Our results suggest that smoothing is best done after differentiating, otherwise high-order derivatives will vanish above the order of the fitting polynomial.⁴⁹

The measured geometrical factors enter the analysis

by the (u,v) method only through $\rho_k(\text{ice})$, and hence only through the comparison sample. The geometrical factor for that sample then acts as a gross scaling factor for $\Delta(T)$, rather than being a highly critical quantity along with the geometrical factor of the alloy sample, for determining, the temperature dependence of $\Delta(T)$. This is a major advantage of this mode of analysis. To test the sensitivity of the (u,v) method to the *temperature dependence* of the geometrical factor of the alloy sample compared with that of the pure comparison sample, the Grüneisen equation for the lattice specific heat was numerically integrated to obtain the change of the thermal expansion coefficient with temperature. This was done for MR6-1, the Pt-Rh sample, and the results are shown by the circular data points in Fig. 5. By comparing them with the uncorrected points it is evident that the thermal-expansion differences are small enough to be neglected.

In the case of the quenched samples the geometrical factor relative to the pure sample can be obtained by electrical resistance measurements prior to quenching to about one order of magnitude higher precision than by length measurements and weighing. The value of the deviation from MR at the ice temperature obtained in this way for the quenched sample MR1-1 is $\Delta(\text{ice}) = 0.0235 \mu\Omega \text{ cm}$, which is within the error limits of the values obtained by the (u,v) method.

IV. EXPERIMENTAL RESULTS

The electrical resistance of ten gold alloys and nine platinum samples was measured as a function of temperature. The initial voltage, current, and thermometer data were analyzed into resistivity versus temperature, which was then listed, plotted, and punched using a FORTRAN program on a CDC 3600 computer. This basic data deck was then treated by several alternative interpretation subroutines, as for

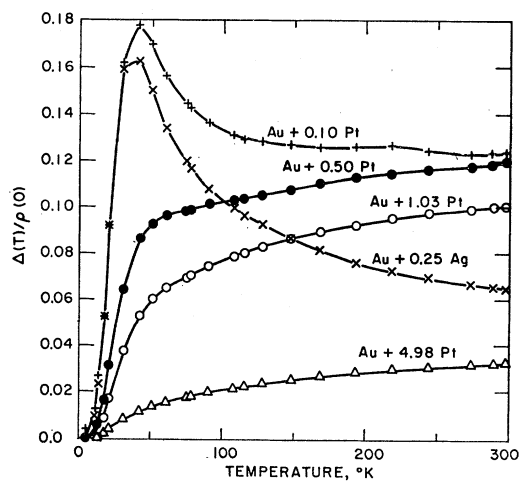


FIG. 6. $\Delta(T)/\rho_0(0)$ versus temperature for a series of gold-platinum alloys and one gold-silver alloy (run MR3).

TABLE I. Gold alloys.

Sample number	Solute	Solute concentration (at.%)	Residual resistivity $\rho(0)$ ($\mu\Omega$ cm)	$\rho(0)/c$ ($\mu\Omega$ cm/at.%)	$\Delta(\text{ice})$ or $\rho(\text{ice})$ ($\mu\Omega$ cm)	Value, rms deviation	$\Delta(\text{ice})/c$ ($\mu\Omega$ cm/at.%)	$\Delta(\text{ice})/\rho(0)$ Value, rms deviation	Low- T power law
MR3-1	Ag	0.25	0.0805	0.32	0.0053 ± 0.0012	0.021	0.066 ± 0.015	2.9	
MR3-2	none	...	0.00158	...	2.042	3.9
MR3-3	Pt	0.10	0.111	1.11	0.0137 ± 0.0018	0.137	0.123 ± 0.016	2.8	
MR3-4	Pt	0.50	0.480	0.96	0.0564 ± 0.0035	0.128	0.117 ± 0.007	3.2	
MR3-5	Pt	1.03	0.980	0.95	0.0971 ± 0.0073	0.094	0.099 ± 0.008	3.2	
MR3-6	Pt	4.98	4.82	0.97	0.1522 ± 0.0110	0.032	0.031 ± 0.002	3.2	
MR4-1	Co	2.1	2.62	1.25	2.42 ± 0.22	1.21	0.923 ± 0.084	3.5	
MR4-2	none	...	0.00196	...	2.033	4.1
MR4-3	Cu	0.10	0.0340	0.34	0.0028 ± 0.0008	0.028	0.082 ± 0.023	3.2	
MR4-4	Cu	0.98	0.222	0.23	0.1152 ± 0.014	0.118	0.520 ± 0.063	3.7	
MR4-5	Ag	0.09	0.0320	0.36	0.0024 ± 0.0009	0.027	0.075 ± 0.028	3.0	
MR4-6	Ag	0.94	0.292	0.32	0.0194 ± 0.0025	0.021	0.0664 ± 0.009	3.3	

TABLE II. Platinum alloys.

Sample number	Solute	Solute concentration (at.%)	Residual resistivity $\rho(0)$ ($\mu\Omega$ cm)	$\rho(0)/c$ ($\mu\Omega$ cm/at.%)	$\Delta(\text{ice})$ or $\rho(\text{ice})$ ($\mu\Omega$ cm)	Value, rms deviation	$\Delta(\text{ice})/c$ ($\mu\Omega$ cm/at.%)	$\Delta(\text{ice})/\rho(0)$ Value, rms deviation	Low- T power law
MR1-1	vac.	0.016 ^a	0.0654	4.0	0.0238 ± 0.002	1.49	0.364 ± 0.031	3.2	
MR1-2	none	...	0.00226	...	9.85	3.6
MR1-3	vac.	0.041 ^a	0.165	4.0	0.0447 ± 0.002	1.09	0.369 ± 0.017	n.a. ^b	
MR2-1	vac.	0.026 ^a	0.107	4.0	0.0260 ± 0.002	1.00	0.243 ± 0.019	2.4	
MR2-2	none	...	0.00146	...	9.81	3.9
MR2-3	vac.	0.026 ^a	0.105	4.0	0.0186 ± 0.002	0.71	0.177 ± 0.019	3.4	
MR6-1	Rh	9.07	6.91	0.76	0.744 ± 0.066	0.82	0.108 ± 0.0096	n.a. ^b	
MR6-2	none	...	0.00249	...	9.89	3.7
MR6-3	Au	0.09	0.432	4.8	0.0412 ± 0.0096	0.46	0.095 ± 0.022	3.4	
MR6-4	Au	0.45	0.960	2.14	0.0848 ± 0.0096	0.189	0.088 ± 0.010	3.4	
MR6-5	Au	0.88	1.57	1.79	0.160 ± 0.018	0.182	0.102 ± 0.012	3.4	
MR6-6	Au	4.84	6.64	1.37	0.452 ± 0.031	0.093	0.068 ± 0.005	3.4	

^a Obtained by assuming $\Delta\rho/c = 4.0 \mu\Omega$ cm/at.-%.^b Not applicable— $\Delta(T)$ versus T cannot be fit by power law.

example the (u, v) method, to obtain the deviations from MR presented here.⁵⁰

Gold Alloys

The gold alloys studied were selected to evaluate the effect of valence and mass differences between the solute atoms and the solvent gold lattice. A synopsis of the characteristics of these alloys is given in Table I. The temperature dependence of the deviations from MR divided by the residual resistivity for the gold-platinum alloys and one gold-silver alloy is presented in Fig. 6. The label on each curve indicates the type and concentration in atomic percent of the solute. The general trend of $\Delta(T)$ is a rapid rise in the temperature interval between 10°K and 30 to 60°K followed by a saturation in the room-temperature range, where $\Delta(T)$

is approximately constant and MR is valid in differential form. A peak at about 40°K is evident in the deviations of the two lowest concentration alloys. It is evident by inspection of the figure that $\Delta(T)$ is not a linear function of solute concentration c . Since $\rho(0)$ was found to be directly proportional to the measured concentration c for the gold-platinum alloys, if $\Delta(T)$ were also proportional to c , the $\Delta(T)/\rho(0)$ loci should superimpose, which they clearly do not. The values of $\Delta(\text{ice})$ and the ratios $\Delta(\text{ice})/\rho(0)$ and their rms deviations, for the different alloys are given in Table I. The rms deviations of $\Delta(\text{ice})$ in Tables I and II are based on approximately 12 variations of the smoothing, curve fitting, and differentiating procedures used in treating the basic data in the (u, v) method of analysis. Figure 6 also shows that 0.1 at.-% Pt in gold yields a larger deviation from MR than 0.25 at.-% Ag. However, the general form of the curves is similar for both solutes.

Figure 7 contains the comparable plots for gold alloys containing cobalt, copper, and silver solutes. The gold-

⁵⁰ Complete tables of $\rho_j(T)$ versus T , and $\Delta(T)$ versus T for all samples, as well as the FORTRAN program listings, are contained in the appendices of the thesis. Copies are available from University Microfilms, Inc., Ann Arbor, Mich.

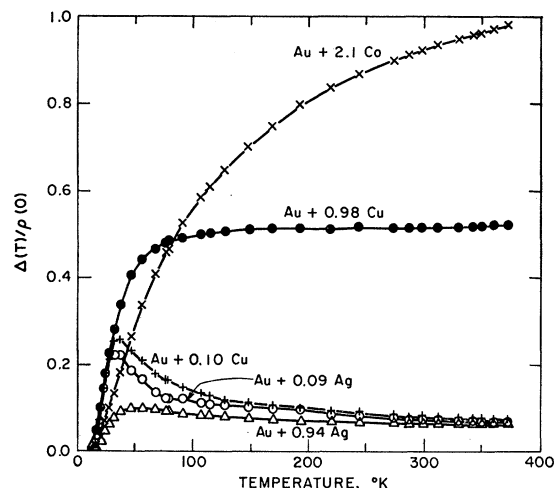


FIG. 7. $\Delta(T)/\rho_0(0)$ versus temperature for gold alloys containing cobalt, copper, and silver as solutes (run MR4).

cobalt alloy is a standard thermocouple alloy. As Table I shows, its room temperature deviation per at.% solute is about 10 times greater than that of the alloy containing 1 at.% copper and comprises one-third of the total room-temperature resistivity. The shape of the curve for the gold-cobalt alloy in the low-temperature range is distinctly different from that of the copper and silver solute alloys. Its temperature dependence is not well matched by a KSW-type equation. It is evident from Fig. 7 that the gold-copper alloys have deviations several times larger than the gold-silver alloys for comparable solute concentrations. Again a distinct peak is evident at about 40°K for the two low concentration copper and silver solute alloys. A broader peak, of approximately the same *absolute* magnitude in $\Delta(T)$ but smaller *relative* magnitude in $\Delta(T)/\rho_0(0)$ exists in the curves for the 0.945 at.% silver solute alloy. The peak in the latter alloy appears to be shifted about 15°K upward in temperature.

A plot of the deviations from MR as a function of solute concentration for the *Au*-Pt alloys at different

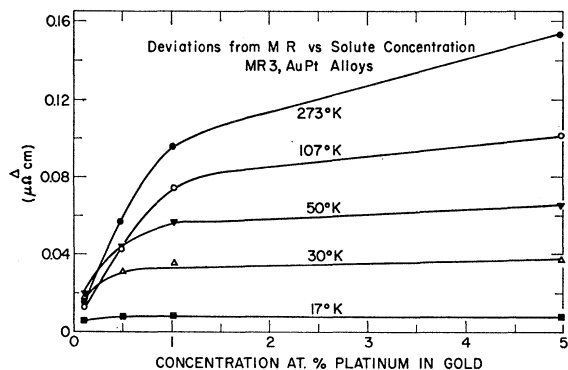


FIG. 8. Deviations from MR at fixed temperatures as a function of solute concentration for gold-platinum alloys (run MR3).

temperatures is given in Fig. 8. It shows that $\Delta(T)$ is nonlinear in solute concentration c . At very low temperatures the deviations are essentially independent of solute concentration. At high temperatures they tend to saturate at a concentration of a few at.%. The low temperature peak is certainly not proportional to solute concentration.

Comparison of our results with previously published deviations from MR for similar gold alloys shows that in some cases significant differences exist. Damon and Klemens³⁰ obtained $\Delta(\text{ice}) = 0.045 \mu\Omega \text{ cm}$ for *Au*-2.6 Cu alloy, whereas, we find $\Delta(\text{ice}) = 0.115 \mu\Omega \text{ cm}$ for a *Au*-1.0 Cu alloy, which is relatively 6.6 times larger. The plot of $\Delta(T)$ versus temperature they give for *Au*-1.0 Pt has a pronounced positive slope and yields $\Delta(\text{ice}) = 0.125 \mu\Omega \text{ cm}$. However, a curve they give for a higher Pt solute concentration alloy, *Au*-1.6 Pt, has a negative slope and a smaller value of $\Delta(\text{ice})$, namely, $\Delta(\text{ice}) = 0.085 \mu\Omega \text{ cm}$. In comparison we find for a *Au*-1.03 Pt alloy, $\Delta(\text{ice}) = 0.097 \mu\Omega \text{ cm}$, and for *Au*-4.98 Pt, $\Delta(\text{ice}) = 0.152 \mu\Omega \text{ cm}$, with a small positive temperature dependence of $\Delta(T)$ in the high-temperature range.

Krautz and Schultz⁷ studied the deviations from MR in a *Au*-1.0 Ag alloy, seeing a sharp peak at 50°K followed by a plateau with $\Delta(\text{ice})/\rho_0(0) = 0.075$, which is in good agreement with the value of 0.066 we obtained for the *Au*-0.94 Ag alloy. Also, the magnitude of the peak found by Krautz and Schultz after subtracting a KSW term in the way mentioned in Sec. I, is about the same as ours. The electrical resistivity in the *Au*-Co system has been measured recently by several authors. Domenicali and Christenson,⁵¹ in studying the effect of transition metal solutes on the electrical resistivity of copper and gold, found a large negative deviation from MR for *Au*-2.1 Co [with $\Delta(\text{ice}) = -1.75 \mu\Omega \text{ cm}$] and *Au*-4.3 Co. At low temperatures Van Den Berg *et al.*⁵¹ and Ford *et al.*⁵¹ found resistance minima in the *Au*-Co system for cobalt concentrations larger than about 0.2 at.%. On the other hand our measurements indicate a *positive* deviation from MR for the sample *Au*-2.1 Co in the temperature range between 1.6 and 373°K. The residual resistivity $\rho_0(0) = 2.62 \mu\Omega \text{ cm}$ we measured for the *Au*-2.1% Co specimen is by a factor of about 4.5 smaller than the value obtained by the authors listed above.⁵¹ This indicates that in our *Au*-Co sample the Co concentration is appreciably smaller than its nominal value or that the Co admixture was precipitated into clusters. The latter possibility seems to be more likely since our specimens had been slowly cooled down after the annealing (Van den Berg *et al.*, Ref. 51).

⁵¹ C. A. Domenicali and E. L. Christenson, *J. Appl. Phys.* **32**, 2450 (1961); G. J. Van den Berg, J. Van Herk, and B. Knook, in *Proceedings of the Tenth International Conference on Low Temperature Physics, Moscow, 1966*, edited by M. P. Malkov, Vol. 4, p. 272; P. J. Ford, T. E. Wall, and J. W. Loram, in *Proceedings of the Eleventh International Conference on Low Temperature Physics* (University of St. Andrews Printing Department, 1968), p. 1246.

Platinum Alloys

The characteristics of the platinum-gold alloys and the quenched platinum samples are given in Table II. The solute concentration of the *Pt-Au* samples given in Table II (and in Figs. 2, 3, and 10) are those stated by the supplier. These samples were also analyzed by neutron activation and yielded for samples MR6-3, MR6-4, MR6-5, and MR6-6 the solute concentrations of 0.107, 0.472, 1.03, and 4.76 at.%, respectively. The vacancy concentration in the quenched samples was deduced from the residual resistivity, $\rho_i(0)$, using the value $\Delta\rho/c = 4 \mu\Omega \text{ cm}/\text{at.}\%$ for the vacancy resistivity (which may be wrong by a factor of 2) given by Huebener.⁵² By comparison, Kraftmaxer and Lanina⁵³ give $\Delta\rho/c = 2.4 \mu\Omega \text{ cm}/\text{at.}\%$. The plots of $\Delta(T)/\rho(0)$ for the quenched platinum samples are given in Fig. 9, and for four platinum-gold alloys and one standard thermocouple platinum-rhodium alloy in Fig. 10. The minimum evident in $\Delta(T)/\rho(0)$ for sample MR1-1 with 0.016 vac. at about 140°K reproduced itself in a second series of measurements. Such curious behavior of $\Delta(T)$ has been observed in the past. For example, Gerritsen and Linde⁹ observed double peaks in *Cu-Mn* alloys. The remainder of the quenched samples shows a definite peak in the deviations from MR in the range 40–60°K, followed by a shallow minimum at 80–100°K and a gradual rise and leveling off at room temperature.

The deviations for the *Pt-Au* alloys in Fig. 10 are quite similar to those of the *Au-Pt* alloys of Fig. 6. Again a peak is evident in the low concentration alloys at about 50°K. Again the transition metal solute alloy, *Pt-Rh*, shows a distinctively different shape in the low temperature range than do the others. Again the solute concentration dependence of the deviations from MR is nonlinear. The similarity of the deviations from MR of the *Au-Pt* alloys to those of the *Pt-Au* alloys is surprising in view of the drastic differences in the electronic band structure of the solvent metals,^{54,55} and the impurity potential. *Further, the low temperature peak in the platinum samples at about 40°K is not shifted by a change in imperfection from a vacancy with a large mass difference relative to the host lattice to a gold atom with virtually no mass difference.*

Low Temperature Dependence of $\Delta(T)$

The columns labeled "Low-*T* power law" in Tables I and II represent the slope n of straight lines fitted to plots of $\log\Delta(T)$ versus $\log T$ in the temperature range below 30°K. Thus n is the power of T in an expression $\Delta(T) = aT^n$, where a is some constant. The same information is given for the resistivity of the pure com-

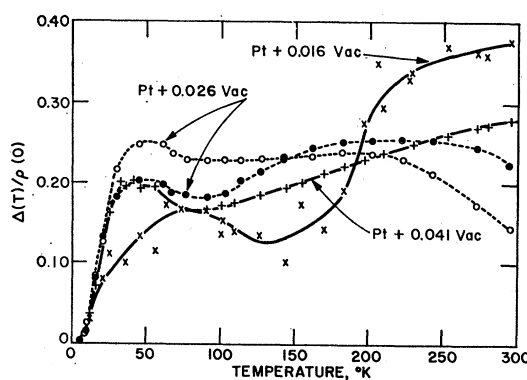


FIG. 9. $\Delta(T)/\rho_i(0)$ versus temperature for lattice vacancies in quenched platinum (runs MR1 and MR2).

parison samples. The tabulated values of n average 3.22 for the deviations from MR of the platinum samples whereas the mean value of n for the resistivity of the pure comparison platinum samples was 3.73. For the gold samples the mean value of n of the deviations was 3.20, whereas that for the resistivity of the pure samples was 4.0. Note that the latter value indicates one power of T less than the Bloch-Grüneisen predicted resistivity temperature dependence of $n=5.0$. It is apparent from the tables that *in every case the value of n obtained for Δ(T) of the impure samples is significantly lower than that for the resistivity of the pure samples*. This implies that an equation of the KSW form [which predicts $\Delta(T) \sim \rho_K(T)$ at low temperatures] is not wholly valid.

Our observed values for n of the deviations from MR are 20% lower than the value $n=4$ suggested by Damon, Mathur, and Klemens.³⁶ Note that this is the same percentage lower that our observed n for ideal lattice resistivity is lower than the Bloch-Grüneisen value. Possibly this may be a consequence of our temperature

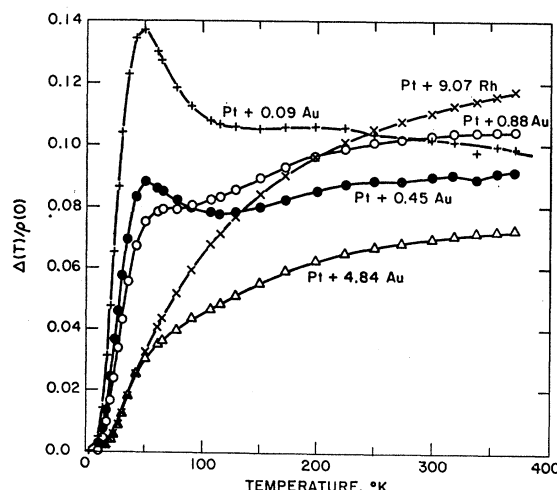


FIG. 10. $\Delta(T)/\rho_i(0)$ versus temperature for platinum-gold and platinum-rhodium alloys (run MR6).

⁵² R. P. Huebener, Phys. Rev. 146, 490 (1966).

⁵³ Ya. A. Kraftmaxer and E. B. Lanina, Fiz. Tverd. Tela. 7, 123 (1965).

⁵⁴ M. D. Stafleu and A. R. de Vroomen, Phys. Letters 19, 81 (1965).

⁵⁵ J. B. Ketterson, M. G. Priestley, and J. J. Vuillemin, Phys. Letters 20, 452 (1966).

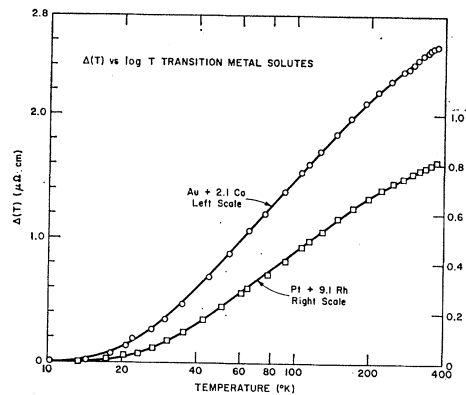


FIG. 11. $\Delta(T)$ versus $\ln T$ for gold-cobalt and platinum-rhodium alloys.

interval (10–30°K) chosen for data analysis which is closer to the linear range of the ideal resistivity than that of Damon, Mathur, and Klemens.

A plot of $\Delta(T)$ versus $\ln T$ is shown in Fig. 11 for the $Au-2.1Co$ and $Pt-9.1Rh$ alloys. The curves for both alloys can be fitted with a straight line from about 30–200°K.

Ratio of Δ (ice) to Residual Resistivity

The ratio of the deviations from MR at 273.2°K to the residual resistivity for the different samples is given in Tables I and II. This ratio, which we shall call α ,⁶ varies over an order of magnitude from 0.031 for $Au-4.98Pt$ to 0.92 for $Au-2.1Co$, or 0.52 for $Au-0.98Cu$, or 0.36 for two Pt -vacancy samples. The ratio α in Au -Cu is noticeably higher than in Au -Ag. Vacancies in Pt cause a relatively higher ratio α than do any of the substitutional element solutes. We note the following dependencies of α with solute concentration c . For Au -Pt and Pt -Au, α decreases with increasing c . For the three Au -Ag alloys, α is approximately independent of c . For the two Au -Cu alloys, α increases by a factor of 6 as c changes from 0.1 to 1%.

V. DISCUSSION

Au , Ag , Cu , and Pt as Solutes

The temperature dependence of the deviations from MR found in the alloys containing Au, Ag, Cu, and Pt as solutes follows approximately a Kohler-Sondheimer-Wilson equation, which predicts a relatively sharp rise of Δ with increasing T at low temperatures and a temperature-independent behavior at high temperatures. Superimposed on this behavior, a sharp peak occurs in the $\Delta(T)$ curves for the low solute concentrations at about 30–50°K. Such a peak has been predicted by Sondheimer⁶ on the basis of higher-order terms in the solution of the Boltzmann equation. The

⁶ α is approximately equal to the constant β in the KSW equation.

contribution to Δ calculated by Sondheimer has a peak at the temperature where the solute resistivity and the impurity resistivity are equal. The peak which is superimposed on a KSW-type behavior in the low solute concentration alloys at low temperatures indeed occurs at the temperature where the residual resistivity approximately equals the ideal resistivity, $\rho_j(0) \approx \rho_k(T)$. The Sondheimer contribution to Δ has an upper limit which is given by the Sondheimer correction term to the electrical resistivity of the solvent metal. This may explain why the low-temperature peak in the $\Delta(T)$ curves occurs only in the low solute concentration alloys and vanishes apparently for higher solute concentrations. In the alloys with higher solute concentrations the Sondheimer contribution to Δ may still exist, but its contribution to Δ may be invisible. Further, because of the condition $\rho_j(0) \approx \rho_k(T)$, the peak shifts with increasing solute concentration to higher temperatures, where the Sondheimer contribution to Δ is relatively small to begin with.

Because of the arguments given above, it appears that the peak in the $\Delta(T)$ curves at low temperatures can be explained by the Sondheimer contribution to Δ superimposed on a KSW-type behavior. Such an interpretation has been given by Krautz and Schultz⁷ to their $\Delta(T)$ curves for $Au-1.0$ Ag and $Ag-0.6$ Au, which showed a similar peak at low temperatures. However, according to Sondheimer the magnitude of the contribution to Δ considered here should be of the order of 1% of the residual resistivity $\rho(0)$. As seen from Figs. 6 and 7, the peak in the additional contribution to Δ can be as high as 20% of $\rho_j(0)$. Alley and Serin⁴⁵ expressed doubt about the existence of the maxima in the $\Delta(T)$ curves reported by Krautz and Schultz. They pointed out that these maxima may represent a fictitious temperature dependence introduced by uncertainties in the geometrical factors of the samples. The present experiments and those of Dugdale and Basinski³³ do not leave any doubt about the existence of these maxima.

Except for the low-temperature maximum in the low solute concentration alloys, the $\Delta(T)$ curves follow approximately the KSW-type behavior indicated in Eq. (3). Assuming that the KSW-type behavior is based on a two-band conduction mechanism as discussed by Sondheimer and Wilson⁵ (including the possibility that different sections of an anisotropic Fermi surface of a single band can act like different bands), the following expressions for the constants β and γ in Eq. (3) can be found⁵:

$$\beta = \frac{1}{\lambda} \left(\frac{\lambda - \mu}{1 + \mu} \right)^2, \quad (20)$$

$$\gamma = \frac{1}{\mu} \left(\frac{\lambda - \mu}{1 + \lambda} \right)^2. \quad (21)$$

Here

$$\lambda = (\sigma_2 / \sigma_1)_{\text{impurity}} \quad (22)$$

TABLE III. Coefficients fit to the KSW equation at T_{low} and T_{ice} .

Sample	Solvent	Solute	T_{low} (°K)	β	γ	λ	μ	λ/μ	General validity of fit
MR1-1	Pt	0.016 Vac.	20	0.371	0.120	0.055	-0.077	- 0.710	poor
MR1-3	Pt	0.041 Vac.	30	0.273	0.602	0.597	0.137	4.34	poor
MR2-1	Pt	0.026 Vac.	20	0.243	0.565	0.520	0.121	4.29	poor
MR2-3	Pt	0.026 Vac.	20	0.176	0.941	0.244	0.031	7.98	poor
MR3-1	Au	0.25 Ag	10	0.067	0.368	0.096	0.015	6.43	fair
MR3-3	Au	0.10 Pt	20	0.123	2.62	0.134	0.005	27.4	fair
MR3-4	Au	0.50 Pt	20	0.120	1.32	0.142	0.010	14.1	good
MR3-5	Au	1.03 Pt	40	0.105	0.783	0.136	0.015	9.32	fair
MR3-6	Au	4.98 Pt	40	0.036	0.602	0.041	0.002	18.0	fair
MR4-1	Au	2.1 Co	20	1.04	9.89	0.870	-0.041	-21.3	fair
MR4-3	Au	0.1 Cu	10	0.083	0.329	0.138	0.028	4.87	poor
MR4-4	Au	0.98 Cu	30	0.529	2.35	0.715	0.062	11.6	very good
MR4-5	Au	0.09 Ag	10	0.075	0.403	0.109	0.017	6.37	good
MR4-6	Au	0.94 Ag	20	0.067	1.74	0.072	0.002	29.8	fair
MR6-1	Pt	9.07 Rh	10	0.149	0.272	0.464	0.159	2.91	very good
MR6-3	Pt	0.09 Au	20	0.096	0.967	0.115	0.009	12.3	fair
MR6-4	Pt	0.45 Au	20	0.089	0.728	0.113	0.011	9.88	good
MR6-5	Pt	0.88 Au	30	0.104	0.672	0.141	0.017	8.09	good
MR6-6	Pt	4.84 Au	40	0.075	0.515	0.099	0.012	8.14	fair

and

$$\mu = (\sigma_2/\sigma_1)_{\text{phonon}} \quad (23)$$

are the ratios of the conductivity in band 2 and band 1 for scattering by impurities and by phonons, respectively. By fitting the experimental $\Delta(T)$ curves with Eq. (3), the constants β and γ have been calculated from the data at or near 20 and 273°K. Subsequently, the parameters λ and μ have been calculated by inverting Eqs. (20) and (21), which yields⁵⁷

$$\lambda = 1 + \frac{1}{2}a \pm \frac{1}{2}a(1 + 4/a)^{1/2} \quad (24)$$

and

$$\mu = 1 + \frac{1}{2}b \pm \frac{1}{2}b(1 + 4/b)^{1/2}. \quad (25)$$

The terms a and b are defined by

$$a \equiv (\gamma - \beta - \beta\gamma)^2 / \beta\gamma^2, \quad b \equiv (\beta - \gamma - \beta\gamma)^2 / \gamma\beta^2.$$

The parameters β , γ , λ , μ , and λ/μ obtained in this way are summarized in Table III. The negative values of γ and μ shown in a few cases are caused by the peak in the $\Delta(T)$ curves at low temperatures, which the KSW equation with constant coefficients cannot fit.

In principle, one can also explain the low-temperature maxima in the $\Delta(T)$ curves for the low solute concentration alloys using the two-band model alone. For this purpose we need only a proper temperature dependence of the coefficients β and γ , and therefore of λ and μ . In the gold alloys we may have a two-band conduction mechanism with the neck region and the belly region of the Fermi surface of gold acting as two individual bands. The required temperature dependence of λ and μ may then result from the temperature-dependent anisotropy of the relaxation time for electron scattering. From Table III we see that for the alloys Au -Pt and Pt - Au $\lambda \gg \mu$ and $1 \gg \lambda$. We can therefore approximate Eqs. (20)

⁵⁷ This form of the inverted Eqs. (20) and (21) has been pointed out to us by B. Lengeler.

and (21) by

$$\beta \approx \lambda \quad \text{and} \quad \gamma \approx \lambda^2/\mu. \quad (26)$$

Finally, we associate σ_1 with the conductivity of the belly region and σ_2 with the conductivity of the neck region. In gold the ratio of the relaxation times for the electron scattering by phonons $(\tau_{\text{neck}}/\tau_{\text{belly}})_{\text{phonon}}$ decreases sharply with decreasing temperature at low temperatures.³⁵ On the other hand, $(\tau_{\text{neck}}/\tau_{\text{belly}})_{\text{impurity}}$ is either constant or only slowly varying with temperature. Therefore, γ decreases sharply with increasing T at low temperatures [Eq. (26)]. If, in addition, $\beta \approx \lambda \sim (\tau_{\text{neck}}/\tau_{\text{belly}})_{\text{impurity}}$ decreases slowly with T at higher temperatures, a maximum in the $\Delta(T)$ curves at low temperatures will arise. Recently, Dugdale and Basinski³³ used precisely this mechanism, namely, the temperature dependence of the anisotropy of the relaxation times, for analyzing their data on deviations from MR in dilute copper and silver alloys. It has been suggested recently^{34,35,58} that the temperature dependence of the ratio $(\tau_{\text{neck}}/\tau_{\text{belly}})_{\text{phonon}}$ causes the observed increase in the Hall constant of the noble metals at low temperatures.

Whereas the arguments given above may favor an interpretation using a two-band model, there are some drawbacks. First, in the two-band model and in the derivation of Eq. (3) it is assumed that no interband scattering occurs between the two bands (or the two sections of the Fermi surface). This, however, is a very unlikely proposition in a system like gold. Second, the two-band mechanism can hardly explain the similarity of the results obtained with the gold and the platinum alloys, since the electronic band structure in Pt is quite different^{54,55} from that in Au.

A mechanism, which yields a KSW-type behavior for $\Delta(T)$ and which is not sensitive to the electronic band

⁵⁸ H. Plate, Physik Kondensierten Materie 4, 355 (1966).

structure of the metal, can be found in the anisotropy of the lattice vibrations as discussed by Bross.²⁸

It was pointed out in Sec. IV that the proportionality $\Delta(T) \sim \rho_{\text{solvent}}(T)$, required by Eq. (3) at low temperatures, is not accurately reflected in the experimental results. This suggests that there are contributions to the deviation Δ which have a temperature dependence lower than that of the ideal resistivity. Since there are typically only about five or six data points in the temperature interval between 10 and 30°K, we do not attempt to strip out the terms of individual powers of T using least square polynomial techniques.

Finally, we examine the aspects arising from the changes in the Fermi energy due to alloying. It is convenient to use the diffraction theory^{59,60} for describing the scattering of electrons within a lattice. The squared matrix element for the transition between the electron states \mathbf{k} and $\mathbf{k}' = \mathbf{k} + \mathbf{q}$ can then be written as

$$|\langle \mathbf{k} + \mathbf{q} | W(\mathbf{r}) | \mathbf{k} \rangle|^2 = S(\mathbf{q}) |\langle \mathbf{k} + \mathbf{q} | w | \mathbf{k} \rangle|^2. \quad (27)$$

$W(\mathbf{r})$ is the (screened) potential at the location \mathbf{r} due to the ions. $W(\mathbf{r})$ is the sum of the contributions of the individual ions at the positions \mathbf{r}_j , $W(\mathbf{r}) = \sum_j w(|\mathbf{r} - \mathbf{r}_j|)$. The structure factor $S(\mathbf{q})$ is given by

$$S(\mathbf{q}) = s^*(\mathbf{q}) s(\mathbf{q}), \quad (28)$$

with

$$s(\mathbf{q}) = \frac{1}{N} \sum_j e^{-i\mathbf{q} \cdot \mathbf{r}_j} \quad (29)$$

(N = number of ions). It depends only upon the ion positions. The form factor

$$\langle \mathbf{k} + \mathbf{q} | w | \mathbf{k} \rangle = \Omega_0^{-1} \int e^{-i(\mathbf{k} + \mathbf{q}) \cdot \mathbf{r}} w(\mathbf{r}) e^{i\mathbf{k} \cdot \mathbf{r}} d\tau \quad (30)$$

(Ω_0 = volume per ion) depends only upon the individual ion potential. The temperature dependence of the structure factor arises through the expansion of the position vector \mathbf{r}_j , or the displacement from an equilibrium position, into a set of normal coordinates, which are populated according to the Bose-Einstein statistics and the frequency distribution function for the specific lattice. Since the vibrational spectrum is usually changed by alloying, the structure factor will then be an explicit function of temperature and solute concentration as well as the momentum transfer variable \mathbf{q} . Under isotropic conditions the relaxation time τ for electron scattering is, for the pure element at finite temperature or an alloy at 0°K, given by

$$\frac{1}{\tau} = C \int_0^{2k_F} S(\mathbf{q}) |\langle \mathbf{k} + \mathbf{q} | w | \mathbf{k} \rangle|^2 q^3 dq, \quad (31)$$

⁵⁹ L. J. Sham and J. M. Ziman, in *Solid State Physics*, edited by F. Seitz and D. Turnbull (Academic Press Inc., New York, 1963), Vol. 15, p. 221.

⁶⁰ W. A. Harrison, *Pseudopotentials in the Theory of Metals* (W. A. Benjamin, Inc., New York, 1966), p. 19.

where C is a constant, and k_F the k value at the Fermi energy. However, the matrix element for alloys at finite temperatures cannot be factored into a structure factor and form factor and cannot yield the simple form of Eq. (31), except in special cases. This arises since the vibrational spectrum as well as the potential can be different at a solute atom site, and since the ideal lattice structure factor is finite for \mathbf{q} not equal to a reciprocal lattice vector and nonzero temperature. Hence, when the matrix element is squared to obtain the transition probability, cross product terms appear which mix the ideal lattice term and the extra terms arising from the change in structure factor and potential at the impurity sites. These extra terms cause deviations from MR as has been discussed by Kagan and Zhernov.³² Only if either the structure factor or the potential of the solute is the same as that of the solvent will the matrix element lead to a factorizable transition probability such that the relaxation time (and so the resistivity) for the alloy can be described by an equation of the form of (31).

Nevertheless, Eq. (31) does provide a basis for discussion in the following sense. The changes in structure factor and pseudopotential for an alloy discussed above, that give rise to deviations from MR, represent changes in the integrand of (31). However, in addition to the changes in the integrand, the surface of integration itself may change upon alloying. This can be due to changes in the Fermi level or Fermi surface based on band-structure and net-charge considerations, or to changes in size of the Brillouin zone itself, if the unit cell dimensions vary with alloying. Since the contribution to deviations from MR arising from the combination of changes in integrand and change in integration contour will be of second order, the first-order term will come from the pure lattice or solvent component of the structure factor and pseudopotential, in which case the factored form of the integrand in Eq. (31) is valid. The contribution to the resistivity due to a shift Δk_F in Fermi momentum is then readily shown to be proportional to

$$\Delta k_F \times 8k_F^3 \times S(2k_F) \times |\langle -\mathbf{k}_F | w | \mathbf{k}_F \rangle|^2. \quad (32)$$

Hence, it will have a temperature dependence corresponding to that of the structure factor evaluated at twice the Fermi momentum. The magnitude of this contribution will be approximately proportional to the pure solvent resistivity. We say approximately since the solvent resistivity is proportional to the integral in Eq. (31), whereas Eq. (32) represents the integrand evaluated at the upper limit. The inference from the mechanism considered here that the deviation from MR should be proportional to the solvent resistivity tends to be supported by our observations that the deviation from MR for the Pt-Au alloys is higher than that for the Au-Pt alloys. According to Eq. (32), the sign of the deviation from MR due to a shift in Fermi energy should be negative if the Fermi surface shrinks upon

alloying. The addition of Pt to Au would lead one to expect a lowering of the Fermi energy as the empty d levels in Pt are filled by the Au s electrons. A compensation arises from the fact that the lattice constant of Pt is smaller than that of Au. Hence, the question of whether k_F increases or decreases is not solely determined by valence considerations. This argument also applies for equivalence alloys, such as Au -Ag and Au -Cu. Since the lattice constant for Cu is smaller than for Au, whereas that of Ag is the same as in Au, one would expect a larger deviation from MR for Au -Cu alloys than for Au -Ag alloys if a change in Fermi energy is important. The experimental results given in Sec. IV indicate that the deviations from MR for Au -Cu are much larger than for Au -Ag, and so tend to support the mechanism based on the change in Fermi energy.

The temperature dependence of the structure factor evaluated at $2k_F$ will not be the same as that of the portions for lower q because of the presence of the Debye-Waller factor, which takes into account multiphonon processes.⁵⁹ The Debye-Waller factor multiplies the remainder of the structure factor by $\exp[-2W^*(q)]$. For a Debye model with cubic symmetry W^* is at high temperatures given by⁵⁹

$$W^* \approx \frac{3}{2} \frac{\hbar^2 q^2 T}{M k_B \Theta^2}. \quad (33)$$

Here M , k_B , and Θ are the ion mass, Boltzmann's constant, and the Debye temperature, respectively. \hbar is Planck's constant divided by 2π . The remainder of the structure factor is proportional to the temperature at high temperatures. Thus, we have at high temperatures

$$S(q) \sim T \exp[-(3\hbar^2 q^2 T / M k_B \Theta^2)]. \quad (34)$$

The low- q part will essentially vary as T , while the negative exponential dominates the high- q part. Thus the structure factor at $q = 2k_F$ can actually decrease with increasing temperature, while the low- q part still increases. If the change in Fermi energy is an important mechanism in the deviations from MR, a plot of $\log[\Delta(T)/T]$ versus T should yield a straight line with a negative slope in the high-temperature range. From the magnitude of the slope the Debye-Waller factor at $2k_F$ can then be calculated. Such a plot is given in Fig. 12 for five platinum alloys. With the exception of the low solute concentration alloy, the figure confirms the linear relation expected. A further expectation is that the magnitude of $\Delta(T)$ should decrease at very high temperatures. The results of Domenicali and Christenson⁵¹ indeed show such a decrease in $\Delta(T)$ above 500°K. A plot of $\log\{\Delta(T)/T\}$ versus T for their Cu -9.46 Mn sample yields a straight line to above 850°K. However, the exponent of the Debye-Waller factor calculated from the slopes of the straight lines obtained in the plots of $\log(\Delta(T)/T)$ versus temperature is found to be about 50 times larger than the value estimated from Eq. (33). Thus, while the functional form of the $\Delta(T)$ curves expected from Eq. (32) for high temperatures

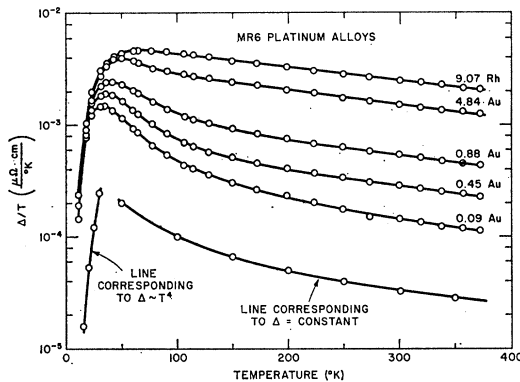


FIG. 12. $\log\Delta(T)/T$ versus temperature for platinum-gold and platinum-rhodium alloys (run MR6).

seems to be in accord with the experimental results for high solute concentration alloys, the numerical agreement with theory is not satisfactory.

In summary it appears that several mechanisms can be suggested for explaining the data qualitatively. Probably the observed deviations from MR are actually caused by several mechanisms simultaneously. Therefore, it seems to be difficult to give an unambiguous interpretation with one single model.

Co and Rh as Solutes

Whereas the Au -Pt alloys were found to behave quite similar to the alloys containing nontransition-metal impurities, the two other transition-metal solutes investigated, cobalt and rhodium, gave quite different results.

As mentioned in Sec. I, magnetic impurities can lead to anomalies in the temperature dependence of the electrical resistivity. In particular, a minimum in the resistivity at very low temperatures is often observed in alloys containing small amounts of magnetic impurities.^{10,11} Recently, Kondo¹² has treated the resistance minimum in dilute magnetic alloys theoretically. He obtained in the resistivity a contribution due to spin scattering of the form

$$\rho_s = c \rho_M [1 + (3zJ/E_F) \ln T], \quad (35)$$

where z is the electron per atom ratio, E_F the Fermi energy, J the s - d exchange integral, and c the atomic fraction of the magnetic ions. ρ_M is given by

$$\rho_M = 3\pi m J^2 s (s+1) V / 2e^2 \hbar E_F N, \quad (36)$$

where m is the electronic mass, s the spin value of the ion, N/V the number of atoms per unit volume, and e the elementary charge. The second term in Eq. (35) gives a negative contribution to the electrical resistivity if the s - d exchange integral J is negative. When combined with the lattice resistivity, this negative term causes a resistance minimum.

According to Fig. 11 a plot of the deviation Δ versus $\ln T$ for the samples *Au*-2.1Co and *Pt*-9.07Rh gives a straight line between about 30 and 200°K. As has been mentioned in Sec. IV, in our *Au*-Co alloy the effective Co concentration may be appreciably smaller than 2.1 at %. This may explain why we did not find negative deviations Δ as has been reported by others for this system.⁵¹ The linearity of both curves shown in Fig. 11 may suggest that between about 30 and 200°K the Kondo term in the resistivity proportional to $\ln T$ is the dominant contribution to Δ . The tailing off in the curves at lower temperatures may be associated with a small contribution to Δ from another mechanism. An inter-

pretation of the curves in Fig. 11 with Kondo's $\ln T$ term would suggest that the *s-d* exchange integral J is positive in both samples. From the slope of the curve shown in Fig. 11, in combination with Eqs. (35) and (36) the value $J=0.6$ eV is then obtained for the sample *Au*-2.1 Co.

ACKNOWLEDGMENTS

It is a pleasure to acknowledge valuable suggestions from R. E. Govednik regarding the experimental procedures. The authors had helpful discussions with C. van Baarle, J. E. Robinson, and O. C. Simpson.

Transition Radiation from an Irradiated Multilayer

S. Y. SHIEH

Department of Physics and Astronomy, University of Tennessee, Knoxville, Tennessee 37916

(Received 29 December 1969)

A general formula for the transition radiation emitted by a uniformly moving charged particle normally incident on a multilayer, either self-supporting or deposited on a thick substrate, is calculated. This formula enables one to take into account the exact multilayer configuration of targets, e.g., oxide layers in the analysis of transition radiation data.

1. INTRODUCTION

TRANSITION radiation, emitted by uniformly moving charged particles crossing the interface of two media having different dielectric properties, has recently been the subject of many theoretical and experimental studies.^{1,2} More recently the construction of a new high-energy particle detector making use of transition radiation is being developed.³ In experimental work, the targets often consist of multilayers, either self-supporting or deposited on a thick substrate, but a general formula which can account for the real configuration of multilayers has not yet been calculated. In this paper, we present the result of an exact treatment of the transition radiation from an arbitrary multilayer due to normally incident charged particles. Since an excellent exposition of the underlying electromagnetic theory and the methods used below is available in Ref. 4, we restrict ourselves to the essential points and the new results in the following concise presentation of the derivation of a general formula for transition radiation from a multilayer.

¹ F. G. Bass and V. M. Yakovenko, *Usp. Fiz. Nauk.* **86**, 189 (1965) [English transl.: *Soviet Phys.—Usp.* **8**, 420 (1965)]. This is the most comprehensive review article up to 1965.

² J. C. Ashley, L. S. Cram, and E. T. Arakawa, *Phys. Rev.* **160**, 313 (1967).

³ L. C. L. Yuan, C. L. Wang, and S. Prünster, *Phys. Rev. Letters* **23**, 496 (1969).

⁴ R. H. Ritchie and H. B. Eldridge, *Phys. Rev.* **126**, 1935 (1962).

2. GEOMETRY OF PROBLEM AND BOUNDARY CONDITIONS

Consider an n layer bounded by the $n+1$ plane interfaces parallel to the xy plane located at $z=D_p$ ($p=1, \dots, n+1$). The thickness d_p of the p th layer between $z=D_p$ and $z=D_{p+1}$ is $d_p=D_{p+1}-D_p$, and its dielectric constant is ϵ_p . The semi-infinite spaces $z \leq D_1=0$ and $z \geq D_{n+1}$ are characterized by dielectric constants ϵ_0 and ϵ_{n+1} , respectively.

When a uniformly moving charged particle passes through the n layer along the normal to the plane interfaces of the n layer, taken as the z axis, the only non-vanishing component of the current density $\mathbf{j}(\mathbf{r},t)=(0,0,j_z)$ and the Hertz vector $\mathbf{H}(\mathbf{r},t)=(0,0,\Pi_z)$ will be the z component and we omit the subscript z below. If the particle carries a charge Ze and moves at velocity v , then the current density is given by

$$j(\mathbf{r},t)=Zev\delta(x)\delta(y)\delta(z-vt). \quad (1)$$

Here we have assumed that the particle crosses the front interface $z=D_1=0$ at time $t=0$ and $\delta(x)$ denotes Dirac's δ function.

The Fourier transform of (1),

$$J(k_x, k_y, \omega | z) = \frac{1}{(2\pi)^{3/2}} \int_{-\infty}^{+\infty} dx \int_{-\infty}^{+\infty} dy \int_{-\infty}^{+\infty} dt \times j(\mathbf{r},t) e^{-i(xk_x + yk_y - \omega t)}, \quad (2)$$